

DETECTION OF ELECTRICAL FAULTS IN INDUCTION MOTOR FED BY INVERTER USING SUPPORT VECTOR MACHINE AND RECEIVER OPERATING CHARACTERISTIC

^{1,2}DIAN R. SAWITRI, ¹I. KETUT E. PURNAMA, ¹MOCHAMAD ASHARI

¹Electrical Engineering Department, Institut Teknologi Sepuluh Nopember, Surabaya, Indonesia

²Electrical Engineering Department, Dian Nuswantoro University, Semarang, Indonesia

E-mail: dianrs@elect-eng.its.ac.id ; ketut@ee.its.ac.id ; ashari@ee.its.ac.id

ABSTRACT

Fault in induction motor is crucial problem in industrial processes. This paper presents the system for electrical fault detection in induction motor fed by inverter. Current spectrum with different frequency is used to fault monitoring. Faults observed includes variation of frequency, unbalance voltage, and inter turn short circuits. Through an experiment, the fault was fired and the current spectrum recorded at steady state condition. Preprocessing is performed before the identification process. It includes noise reduction using wavelet analysis and feature extraction with Principal Component Analysis (PCA). Both processes are intended to eliminate the noise, reducing the dimension of feature, and retrieve components of the optimal features for classification. Strength of identification capability using Support Vector Machine (SVM) is 83.51%. Based on the ROC (Receiver Operating Characteristic) analysis, the SVM classifier has a good enough performance. This is indicated by the sensitivity is 74.31%, specificity is 47.30% and *G-Mean* is 1.1028.

Keywords: *Electrical Fault Detection, Induction Motor, Principal Component Analysis (PCA), Receiver Operating Characteristic (ROC), Support Vector Machine (SVM).*

1. INTRODUCTION

Induction motor is widely used in industrial application. During operation, the motor may be experience with faults. If the fault is not treated then the motor may have failed that causes production activities must be stopped. So, the production process disrupts and causes energy waste.

Fault in induction motor can be either mechanical or electrical fault. In the previous study, the detected fault in induction motor are broken rotor bar [1]-[4] and bearing fault [1],[4]-[6]. Electrical fault is usually influenced by power quality that supplied by ac grid, such as variations of frequency and unbalanced voltage. Another fault is intern short circuits in stator winding [1],[7]-[10]. Some study has applied artificial transform as denoising algorithm [11]. For multidimensional data, wavelet transform will be combining with Principal Component Analysis (PCA) as denoising algorithm [12]. Observed signal usually contain many parameter feature. To

intelligent method to detect the both of fault. The methods are fuzzy logic [6][10], Fast Fourier Transform (FFT) [3],[5],[6],[8], Artificial Neural Network (ANN) [7], Support Vector Machine (SVM) [4], and Kalman Filter [2].

Motor Current Spectrum Analysis (MCSA) is used as fault parameter in the motor. In industrial applications, induction machines are supplied and controlled by inverters. The effect of the inverters causes the high harmonics in the currents that were recorded due to the switching operation. Thus, it becomes more difficult and demanding to detect faults by using MCSA in this drives [3]. To get a more accurate identification, need to be done several processes to reduce the noises and eliminate features that are not desirable. Current spectrum with high noises can reduced with wavelet

increase the identification, feature extraction need to be done on original signal. Feature extraction is performed to eliminate the feature parameter that are not appropriate and reduce the dimensional of data [13]. Feature extraction methods have been

used in previous study to improve the classification accuracy. The methods are Independent Component Analysis (ICA) [4]-[6], Kernel ICA, PCA, and Kernel PCA [6].

This study detected the electrical fault in induction motor fed by inverter. The faults are caused by variation of frequency, unbalance voltage, and inter-turn short circuits. The effect of fault and inverter in this research caused the high noise. To reduce the noises, combination wavelet and PCA are used as denoising algorithm. Feature extraction with PCA and SVM classification with ones-against-ones strategy selected to identify the fault condition.

The Performance of SVM as classifier will be determined by Receiver Operating Characteristic (ROC). In most previous studies, ROC analysis were applied on pattern recognition to diagnose a disease [14],[15]. The ROC Analysis for power system research has been tested to examine of fault identification on a radial distribution system with SVM [16]. In this paper, we use ROC analysis to determine the performance of SVM classifier for fault identification system on induction machine fed by inverter.

2. METHODS AND EXPERIMENT

2.1 The Fault Identification System

The block diagram or lab test bench of the proposed fault identification system is shown in Fig. 1. The characteristics of the three-phase induction motor used in this experiment are listed in Table I. The Current spectrum is recorded from the motor caused driven by inverter. The faults were raised by varying the frequency of inverter, unbalance voltage, and inter turn short circuits.

TABLE I
MOTOR CHARACTERISTIC USED IN EXPERIMENT

Description	Value
Power	0.25 kW
Input Voltage	380 V
Full Load Current	0.82 A
Suply Frequency	50 Hz
Number of Poles	4
Full Load Speed (rpm)	1320

Fault identification consists of 4 steps that are: denoising, feature calculation, feature extraction, and classification. To determine the validity of classifier, the step is resumed by analyzing the performance of classification.

2.2 Denoising Signal

Noise from current spectrum with high harmonic must be removed by filtering or denoising. Combination of wavelet transform and Principal Component Analysis (PCA) is used as de-

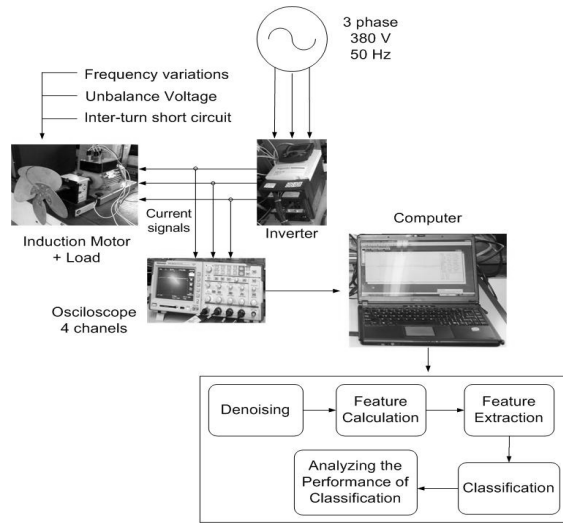


Fig. 1. The proposed fault Identification System

noising algorithm [12]. In general, the recorded signal is modeled as follows:

$$x(t) = f(t) + \varepsilon(t) \quad t = 1, \dots, n \quad (1)$$

Where $x(t)$ is observed signal, $\varepsilon(t)$ is a centered Gaussian white noise of unknown variance and $f(t)$ is a unknown function to be recovered through the observations (Fig. 2)

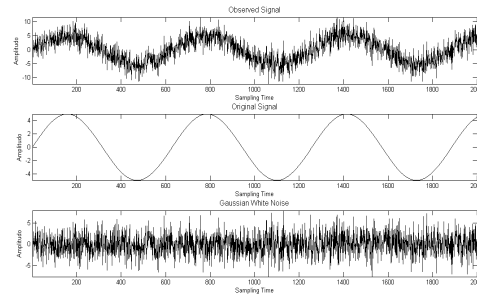


Fig. 2. Observed Signal, Original Signal, and Gaussian White Noise

Denoising procedure combining wavelet and PCA is applied to reduce noise in multichannel signal recording [12]. The scheme is as follows:

- 1) Perform the wavelet transform at level J of each column of x [12]-[13]
In this step, the orthogonal wavelet is decomposed to Detail signal (D_j) and Approximation signal (A_j). The orthogonal

wavelet consists of *scaling function* ($\phi(x)$) and *wavelet function* ($\psi(x)$) (2).

$$\phi(x) = \sum_{t=0}^{J-1} a_k \phi(2x - t) \quad (2)$$

$$\psi(x) = \sum_{t=0}^{J-1} b_k \phi(2x - t)$$

Where $(a_0 - a_{J-1})$ is scaling sequence and $(b_0 - b_{J-1})$ is wavelet sequence. Scaling functions are associated with low-pass filters with coefficient $\{h(n), n \in \mathbb{Z}\}$, while wavelet functions are associated with high-pass filters with coefficient $\{g(n), n \in \mathbb{Z}\}$, (Fig 3).

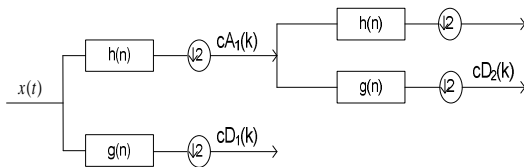


Fig. 3. Two Level Filter Bank Decomposition Wavelet

In this way, the decomposition coefficient can be described as (3):

$$\begin{aligned} [x(t)] &\leftrightarrow [cA_1, cD_1] \\ &\leftrightarrow [cA_3, cD_3, cD_2, cD_1] \\ &\leftrightarrow \dots \end{aligned} \quad (3)$$

- 2) For $1 \leq j \leq J$, perform the PCA of the matrix cD_j and select an appropriate number p_j of useful principal component or suppress the detail cD_j ;
- 3) Similarly, perform the PCA from the matrix cA_j and select p_{j+1} principal component;
- 4) From the simplified detail and approximation matrices reconstruct a new matrix \tilde{x} containing the main features of the original matrix x , by inverting the wavelet transform;
- 5) Finally perform the PCA of the matrix \tilde{x} .

2.3 Feature Calculation and Feature Extraction

After denoising, feature parameters are calculated based on time domain and frequency domain. There are 25 feature parameters of each phase (phase R, S, and T). We have 10 conditions and each one has 20 measurements, so the total obtained 200 data calculated. The value of features parameter calculated based statistical value of time domain and frequency domain, such as mean, RMS, variance, peaks, moment, entropy, crest factor, Total Harmonic Distortion, etc.

We used PCA as feature extraction algorithm [17]-[18]. PCA will reduce the dimension of parameter but not eliminate the information about the signal. The result is a parameter called Principal Component. The procedure involves eigenvalue and eigenvector as follows:

1. Given a set of n dimension input vector and each of which is of m dimension.

$$x(t) = \begin{bmatrix} x_{11} & x_{12} & \dots & x_{1n} \\ x_{21} & x_{22} & \dots & x_{2n} \\ \dots & \dots & \dots & \dots \\ x_{m1} & x_{m2} & \dots & x_{mn} \end{bmatrix} \quad (4)$$

2. Subtracting the value of each cell x_{ij} with an overall mean μ_j

$$u_j = \frac{1}{m} \sum_{i=1}^m x_{ij} \quad (5)$$

$$\phi_{ij} = x_{ij} - \mu_j \quad (6)$$

3. Calculate the matrix covariance C

$$C = (x_{ij} - \mu_j)(x_{ij} - \mu_j)^T \quad (7)$$

4. Getting the eigenvalue λ and eigenvector u of matrix covariance C

$$\lambda_i u_i = C u_i \quad (8)$$

Where λ_i is eigenvalue of C , u_i is the corresponding eigenvector.

5. Based on the estimated u_i , the components of s_t are the orthogonal transformations of x_t

$$s_t(i) = u_i^T x_t \quad (9)$$

$s_t(i)$ are called principal components. Dimensional reduction of parameters is executed in (9). By using a specific threshold of the eigenvector, u_i , the dimension of the final data can be determined.

2.4 Classification

In this study, Support Vector Machine (SVM) is used to identify fault of induction motor. All the measured data are classified into 10 types of fault. From each type, it is selected 30% measurement as training and 70% as testing data.

SVM maps the input vectors x into a high-dimensional features space Z through some nonlinear mapping [19]. In this space, an optimal separating hyperplane is constructed (Fig. 4).

The learning machines construct the decision functions that are nonlinear in the input space,

$$f(x) = \text{sign} \left(\sum_{\text{supportvectors}} y_i \alpha_i K(x_i, x) - b \right) \quad (10)$$

To find the coefficients α_i in the separable case (analogously in the non-separable case) it is sufficient to find the maximum of the functional.

$$W(\alpha) = \sum_{i=1}^n \alpha_i - \frac{1}{2} \sum_{i,j} \alpha_i \alpha_j y_i y_j K(x_i, x_j) \quad (11)$$

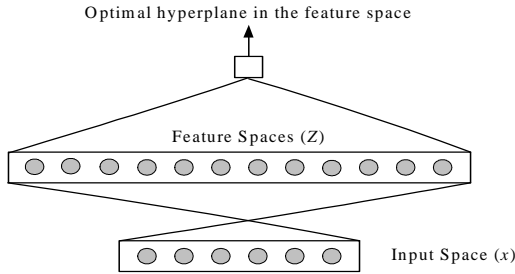


Fig. 4 The SV Machine maps the input space into a high-dimensional feature and then constructs an Optimal hyperplane in the feature space

Subject to the constraints

$$\sum_{i=1}^n \alpha_i y_i = 0 \quad \alpha_i \geq 0, \quad i = 1, 2, \dots, n \quad (12)$$

$K(x_i, x)$ is the Kernel function in input space that equivalent with inner product in feature space. K is a symmetric positive definite function which satisfies Mercer's condition.

$$K(x_i, x) = \sum_{k=1}^{\infty} a_k \psi_k(x_i) \psi_k(x) \quad a_k > 0 \quad (13)$$

It is necessary and sufficient that the condition

$$\iint K(x_i, x) g(x_i) g(x) dx_i dx > 0$$

Be valid for all $g \neq 0$ for which

$$\int g^2(x_i) dx_i < \infty$$

Examples of such kernels are given in Table II.

TABLE II
EXAMPLE OF KERNEL FUNCTIONS

No	Kernel Type	Functions
1	Polynomial	$K(x_i, x) = \langle x_i, x \rangle^d$
2	Gaussian Radial Basis Function	$K(x_i, x) = \exp\left(-\frac{\ x_i - x\ ^2}{2\sigma^2}\right)$
3	Exponential Radial Basis Function	$K(x_i, x) = \exp\left(-\frac{\ x_i - x\ }{2\sigma^2}\right)$
4	Fourier Series	$K(x_i, x) = \frac{\sin\left(N + \frac{1}{2}\right)(x_i - x)}{\sin\left(\frac{1}{2}(x_i - x)\right)}$

The optimal hyperplane separated without error and the distance between the closest vector to the hyperplane is maximal (Fig. 5). Suppose the training data

$$(x_i, y_i), \dots, (x_l, y_l), \quad x \in R^n, \quad y \in \{+1, -1\}$$

Can be separated by a hyperplane :

$$(w, x) + b = 0 \quad (14)$$

where, w and b shall be derived in such a way that unseen data can be classified correctly. To describe the separating hyperplane, the following canonical form can be use:

$$(w \cdot x_i) + b \geq 1 \quad \text{if } y = +1,$$

$$(w \cdot x_i) + b \leq -1 \quad \text{if } y_i = -1.$$

In the following we use a compact notation for these inequalities:

$$y_i [(w \cdot x_i) + b] \geq 1, \quad i = 1, \dots, n \quad (15)$$

It is easy to check that the optimal hyperplane is the one that satisfies the condition (15) and minimizes (Fig. 5).

$$\Phi(w) = \|w\|^2 \quad (16)$$

(The minimization is taken with respect to both vector w and scalar b)

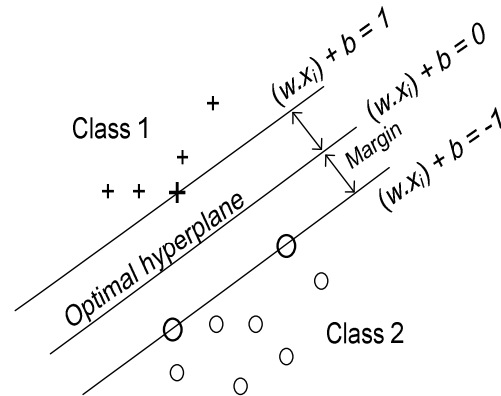


Fig. 5. The Optimal separating hyperplane is the one that separates the data with maximal margin.

2.5 Analysis the Performance of Classification

Classification performance can be analyzed by graph Receiver Operating Characteristic (ROC). ROC graph is a technique to visualize, organize, and choose the type of classification based on its performance [20].

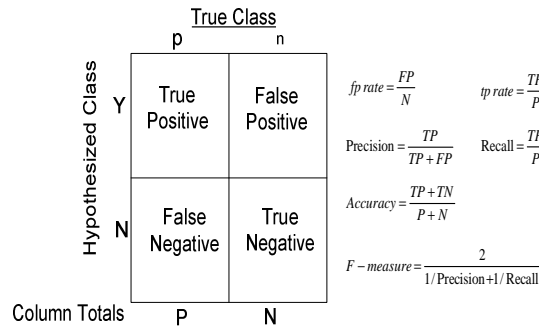


Fig. 6. Confusion matrix and common performance matrix calculated from it

Classification performance is determined by confusion matrix. In binary classification, the outcomes are labeled either as positive (p) or negative (n) class. There are four possible outcomes from a binary classifier. They are *true positive*, *false negative*, *true negative*, and *false positive* (Fig 6). For example, to determine weather a signal has a certain fault. A *true positive* in this case occurs when the signal test is positive (fault) and actually it is positive. A *false positive*, on the other hand, occurs when the test is positive and actually it is negative, similarly for *true negative* and *false negative*.

Fig 6 shows a confusion matrix and equations of several common that can be calculated from it. The numbers along the major diagonal represent the correct decisions made, while the numbers in this diagonal represent the errors —the confusion — between the various classes.

Performance of a classifier can be caused by the imbalance data set. Evaluation the imbalanced classification based on confusion matrix in Fig. 6. There are two kinds of metrics to deal with class imbalanced [21].

The first metrics to obtain an optimal balanced classification ability are *sensitivity* (17), *specificity* (18) and *G-Mean* (19). There are usually adopted to separately monitor the classification performance on two classes. *G-Mean* is the geometric mean of sensitivity and specificity (19).

$$sensitivity = \frac{True\ Positive}{(True\ Positive + Fals\ Negative)} \quad (17)$$

$$specificity = \frac{True\ Negative}{(True\ Negative + Fals\ Positive)} \quad (18)$$

$$G - Mean = \sqrt{sensitivity + specificity} \quad (19)$$

The second metrics are *precision*, *recall*, and *F-Measure* (Fig. 6). Notice that recall is the same as sensitivity. F-Measure is used to integrate precision and recall into a single metric.

3. RESULT AND ANALYSIS

Lab experiments have been done and result in recorded signal of 10 fault conditions with 20 measurements every condition. To identify the fault, it is conducted steps as mentioned in previous section that are denoising process, feature calculation, feature extraction, and classification.

3.1 Denoising Result

Current signal are recorded in this study and have a very high noise. This noise must be removed to avoid bias. Fig. 7 shows example 4 types of three phase current signals that have been filtered using combination of wavelet and PCA. The current signals include normal (no-fault, inter-turn short circuit, and 5% and 10% unbalanced voltage condition).

As seen in Fig.7, combination of wavelet and PCA eliminate the noises. To distinguish the current signal due to unbalance voltage 5% and 10% is difficult, because the spectrum seems very similar. It needs a tool to quickly and accurately recognize faults using the step as describe in previous section.

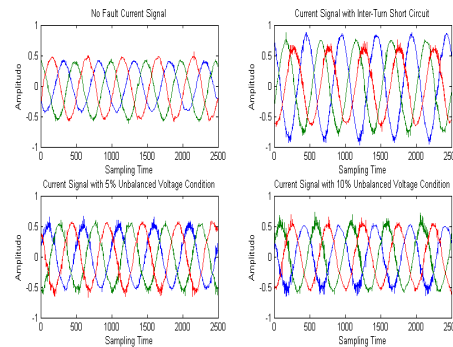


Fig. 7. Denoising Current Signal with Combination of Wavelet and PCA.

3.2 Feature Calculation and Feature Extraction Result

Figure 8 shows the eigenvalue of 25 feature parameters. Only 14 of 25 parameters are selected as principal components to be identified. Selection is based on the high enough eigenvalue. The others are discarded, due to too small.

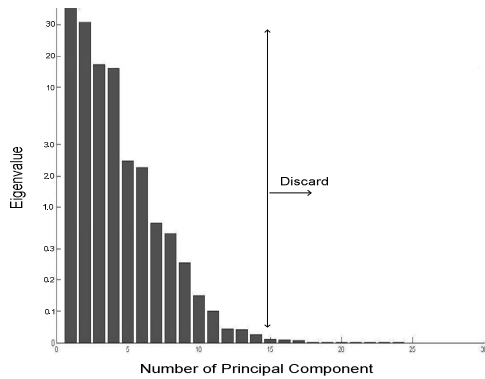


Fig 8. Eigenvalue of Covariance matrix for Feature Selection

In order to show the scatter diagram of faults belongs to each principal component, the 3 biggest eigenvalues of principal components is selected. Fig. 9 shows the scatter diagram of extracted 3 principal component using PCA. As can be seen, the data tends to distribute in a group based on the fault types.

3.3 Identification Result and It's Performance

Fault identification of 14 principal components using SVM method is presented in Table III. The normal condition of 50 Hz frequency can be identified perfectly, presenting 100% of the strength of identification index. The average in 83.51%.

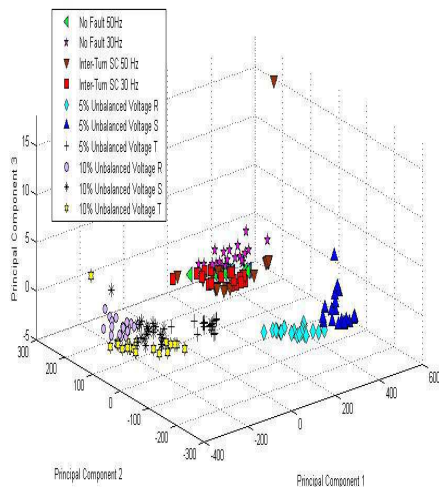


Fig. 9 Scatter Diagram for 3 Largest Principal Component

TABLE III
IDENTIFICATION RESULT USING SVM

Fault Condition	Frequency (Hz)	Strength of Identification (%)
No Fault	50	100
No Fault	30	93.85
Inter-Turn Short Circuits	50	72.31
Inter-Turn Short Circuits	30	84.62
Average 5% Unbalance Voltage	50	81.28
Average 10% Unbalance Voltage	50	68.97
Average		83.51

The performance of SVM classifier is based on ROC analysis, determined in Fig. 10 and Table IV. As seen in Fig. 10, there are 1561 Positive sample (P) and 389 Negative samples (N). There are 1160 samples of 1561 demonstrating a correct identification (True Positive), while 401 samples are False Negative (FN). FN means that the system has no faults, but it was recognized having fault. On the other hand, FP is a resent of SVM identification that system has faults, but it was recognized normal condition.

		True Class	
		p	n
Hypothesized Class	Y	TP = 1160	FP = 205
	N	FN = 401	TN = 184
Column Total		P = 1561	N = 389

Fig. 10 Confusion Matrix of Fault Identification

Table IV shows Sensitivity or TP rate as 0.7431. This indicates the system ability to recognize true signal as 74.31%. However, the ability of system to recognize a wrong signal as specificity is 47.30%. It is calculated from the ratio of TN and total negative samples. Other parameter is found as precision, which is 84.98% calculating from Fig. 6.

TABLE IV
PERFORMANCE OF SVM CLASSIFIER BY ROC

No	Variable	Prob. Value
1	Sensitivity = TP rate	0.7481
2	Specificity	0.4730
3	Precision	0.8498
4	G-mean	1.1028

The Geometric mean (G-Mean) is presented as 1.028. It represents the balanced result between

sensitivity and specificity. G-mean is evenly balanced when the value is 1.0. A better G-Mean is obtained if the value is greater than 1.0.

4. CONCLUSION

Electricity faults in induction motor in this study are identified by SVM based on current signal. The current signals are very noisy since they are generated from a small rate of equipment. Before the process of identification, it is necessary to pre-process the recorded signals for accurate improvement. This includes, denoising signal with combination of wavelet and PCA, feature calculation based on time and frequency domain, and feature extraction using PCA. The study present was 4 principal components of 25 feature parameters based on its eigenvalue. The faults of induction motor are identified by SVM with strength of identification index average in 83.51%. Based on ROC analysis, the ability of system recognizes the true signal is 74.31% (sensitivity) and the wrong signal is 47.30% (specificity). G-Mean is balanced because the value is greater than 1.0.

In the future, current signals from bigger rate of equipment will be observed with more types of fault. To improve the performance of SVM considers improving the feature extraction and feature selection algorithm.

REFERENCES:

- [1] P.J. Travner, "Review of condition monitoring of rotating electrical machines, IET Electrical Power Application", 2008, Vol. 2, No. 4, pp. 215-247
- [2] F. Karami, J. Poshtan, and M. Poshtan, "Detection of broken rotor bars in induction motors using nonlinear Kalman Filters", ISA Transaction, 49, (2010), pp. 189-195.
- [3] I. P. Georgakopoulos, E.D. Mitrokinas, and A.N. Safacas, "Detection of induction motor faults in inverter drives using inverter input current analysis", IEEE Transaction on Industrial Electronic, Vol. 55, No. 9, September 2011, pp. 4365-4373.
- [4] A. Widodo, Bo-Suk Yang, Dong-Sik Gu, and Byeong-Keun Choi, 2009, "Intelligent fault diagnosis system of induction motor based on transient current signal", Mechatronics, 19, (2009), pp. 680-689.
- [5] Zhaoxia Wang, C.S. Chang, and Yifan Zhang, "A feature based frequency domain analysis algorithm for fault detection of induction motors", 2011, 6th IEEE conference on Industrial Electronic and Application
- [6] T. W. Chua, W.W. Tan, Z-X. Wang, and C.S. Chang, "Hybrid time frequency domain for inverter-fed induction motor fault detection", IEEE International Symposium on Industrial Electronic (ISIE), 4-7 July, pp.1633-1638.
- [7] V. N. Ghate and S. V. Dudul, "Optimal MLP neural network classifier for fault detection of three phase induction motor", Expert System with Applications, 37, (2010), pp. 3468-3481.
- [8] R. Sharifi, and M. Ebrahimi, "Detection of stator winding faults in induction motors using three-phase current monitoring", ISA Transactions, 50, 2011, pp. 14-20.
- [9] A. Cakir, H. Calis, E.U. Kucuksille, "Data mining approach for supply unbalance detection in induction motor", Expert System with Applications, 36 (2009), pp. 11808-11813
- [10] V. J. Rodriguez, and A. Arkkio, "Detection of stator winding fault in induction motor using fuzzy logic", Applied Soft Computing, 8, (2008), pp. 1112-1120.
- [11] D.L. Donoho, "De-Noising by soft thresholding", IEEE Transaction on Information Theory, Vol. 41, No. 3, May 1995, pp. 613-627.
- [12] M. Aminghafari, N. Cheze, and J.M. Poggi, "Multivariate denoising using wavelet and principal component analysis," Computational Statistic & Data Analysis 50 (2006), pp. 2381-2398.
- [13] C. Gargour, M. Cabrea, V. Ramachandran, and J.M. Lina, "A Short Introduction to Wavelet and Their Applications", IEEE Circuits and System Magazine, 2nd Quarter , 2009.
- [14] Xin He, Xiyun Song, Eric C. Frey, Application of Three-Class ROC Analysis to Task-Based Image Quality Assessment of Simultaneous Dual-Isotope Myocardial Perfusion SPECT(MPS), IEEE Transaction on Medical Imaging, Vol. 27, No. 11, Nopember, 2008.
- [15] Xin He, Charles E. M., Benjamin M. W. T., Jonathan M. L., and Eric C. Frey, Three Class ROC Analysis – A Decision Theoretic Approach Under the Ideal Observer Framework, IEEE Transaction on Medical Imaging, Vol. 25, No. 5. May, 2006.



- [16] D. R. Sawitri, A. Muntasa, K. E. Purnama, M. Ashari, and M. H. Purnomo, "Data Mining Based Receiver Operating Characteristic (ROC) for Fault detection and Diagnosis in Radial Distribution System, The Journal for Technologi and Science IPTEK, Vol. 20, No. 4, Nopember, 2009.
- [17] L. I. Smith, "A Tutorial Principal Component Analysis", University of Otago, New Zealand, 2002, www.cs.otago.ac.nz/cosc453/student_tutorials/principal_components.pdf.
- [18] I.J. Jolliffe, Principal Component Analysis, Springer, New York, 1986.
- [19] V. N. Vapnik, "The Nature of Stastitical Learning Theory", Springer – Verlag New York, Inc., 1995.
- [20] T. Fawcett, "An Introduction to ROC analysis", Pattern Recognition Letters, 27, 2006, pp 861 – 874
- [21] Yuchun Tang, Yan-Qing Zhang, N. V. Chawla, and S. Krasser, "SVMs Modelling for Highly Imbalanced Classification", IEEE Transaction On System, Man, and Cybernetics – Part B: Cybernetics, Vol. 39, No. 1, February, 2009